Supplementary Information to:

Expanding the Ruddlesden-Popper manganite family: the $n = 3$ $La_{3.2}Ba_{0.8}Mn_3O_{10}$ ferrimagnet.

Joke Hadermann[1], Artem Abakumov[1,3], Alexander A. Tsirlin[2], Marina G. Rozova,[3] Eleni Sarakinou[1,4], Evgeny V. Antipov[3]

Determination of the space group as being Cccm

1. The Fourier transforms (FT) on Figure 2 are shown again below in Figure S1, indexed using the cell parameters $a \approx 29$ Å, $b \approx c \approx 5.6$ Å($= a_p\sqrt{2}$) (a_p is the cell parameter of the perovskite structure). From these two FT it can be deduced that:

   h0l:h=2n, l=2n (from zone [010])

   hk0: h+k=2n (from zone [001])

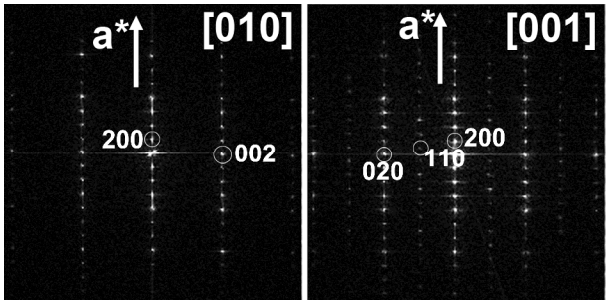

Figure S1. Fourier transforms taken from the HRTEM image shown in Figure 2 in the main text.

2. Since the [100] zone cannot be used for determination of refletion conditions, because it will contain contributions from all intergrowths present, a tilt series around the a*-axis was performed which allows to deduce 0kl reflections from the different [0vw] zones. These [0vw] zones are shown below in Figure S2. From each zone, one combination of k and l can be deduced, from [012] you can derive whether 02-1 is extinct or not, from [013] you can conclude about 0-31 and so on. This gives: 0-24 and 0-22 present, 0-13, 0-12, 0-11 extinct. This leaves two possibilities for 0kl, i.e. either the reflection condition is 0kl: k=2n or it is 0kl: k=2, l=2n. To decide between these two one needs to find whether the reflection 021 (or 0-21) is extinct. If so, the reflection condition is 0kl: k=2n, l=2n, if not, then the reflection condition is 0kl: k=2n. This could not be decided from this same tilt series: the [012] zone was only found in overlap with its twin [021] as shown in Figure S3 on the left side, and in this pattern the 0-21 reflection is present but can be due to double diffraction. However, this reflection node is also present in the [11-2] zone which we used for the refinement, shown in Figure S4. From the indexation presented in the scheme accompanying that figure, one can see that 021 is clearly extinct. Therefor for this compound we have **0kl: k=2n, l=2n**.

3. From all zones together (Figures S1, S2, S3, Figure 1), it can be deduced that the general reflection condition is **hkl: h+k=2n**.

4. Combining these four conditions **hkl: h+k=2n; h0l: h=2n, l=2n; hk0: h+k=2n; 0kl: k,l=2n allows only one possible extinction symbol: Ccc-.** From the space groups possible for this extinction symbol, Ccc2 and Cccm, we used the most symmetric one Cccm, since there was no indication that the symmetry should be lowered to an acentric cell.

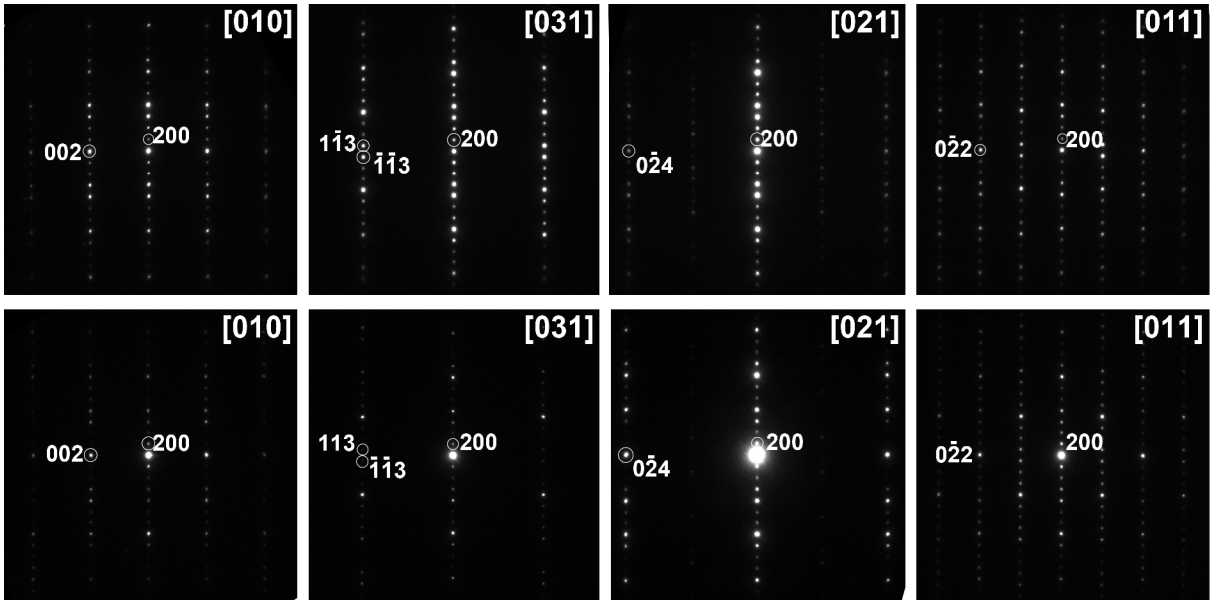

Figure S2. Tilt series around the a*-axis, to determine the 0kl reflection condition. Top row shows selected area electron diffraction patterns, bottom row show precession electron diffraction patterns of the same zones.

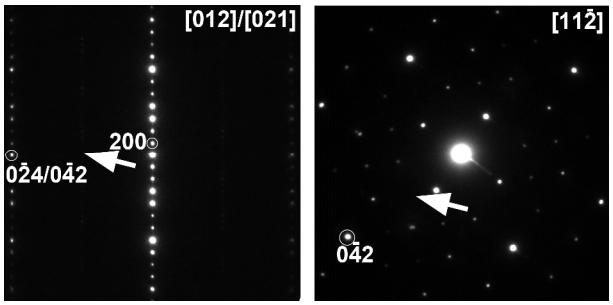

Figure S3. Left: twinned pattern containing [021] plus [012]; right: [11-2] zone (the full indexation scheme of this pattern can be found in Figure S5). An arrow points in both patterns at the position of the 0-21 reflection.

Details on the PED data treatment.

The PED patterns that were used for the refinement are shown in Figures S4-S7. It was checked by simulating the PED patterns in JEMS that there is no overlap with reflections from higher order Laue zones. The intensities of the reflections in the zones with superstructure reflections (the first three zones, shown in Figures S4-S6) could not be extracted using ELD in a conventional manner (i.e. index three reflections and ELD extracts all intensities on the network of lattice points defined by these three indexed reflections), since the obtained PED patterns contained superstructure reflections originating from more than one zone, and also reflections very close together, so automatic indexation led to errors in the indexation. Therefore, the 2D intensity maps (ELD) of the PED patterns with superstructure reflections were analysed. These maps contain the intensities of each separate pixel in the PED pattern and for each undubiously recognizable superstructure reflection the peak intensity was written down manually. It was verified that for the subcell reflections this gave results close to values obtained in the conventional, automated manner, therefore it is assumed to be reliable also for those reflections which cannot be extracted in an automated manner. All these intensities were then typed into an hkl-Intensity list, one for each zone. The zones not containing superstructure reflections were treated in the conventional manner in ELD. Subsequently, the quality of the orientation of the PED patterns was checked using the R_{sym} value (TRIPLE), which gave very good values for each zone (Table S1 in the supporting information). The

intensities were corrected using the geometrical correction factor that takes into account the different coverage of reflections close to the central beam and reflections far away from the central beam such that the new intensity I' equals I'= I.C(g,R)=I.g(1-(g/2R)^2)$^{1/2}$ (where g is the reciprocal vector, and R is the radius of the Laue circle). (1) Taking into account two possible twin variants of the pseudo-tetragonal orthorhombic unit cell, the intensities of the *hkl*: $k + l \neq$ 2n superlattice reflections were increased by a factor of 2. This doubling assumes a 50%-50% presence of both twins, this is supported by the different HRTEM images that were taken of the compund along the direction [010]/[001].

Remark that the patterns were not merged since they were not used for Direct Methods, but they were used for the refinement of the structure in Jana2006. Jana2006 allows the refinement of the structure agains the individual patterns, by considering the scale factors of the patterns as extra refineable parameters.

(1) Gemmi, M.; Nicolopoulos, S. *Ultramicroscopy* **2007**, *107*, 483–94.

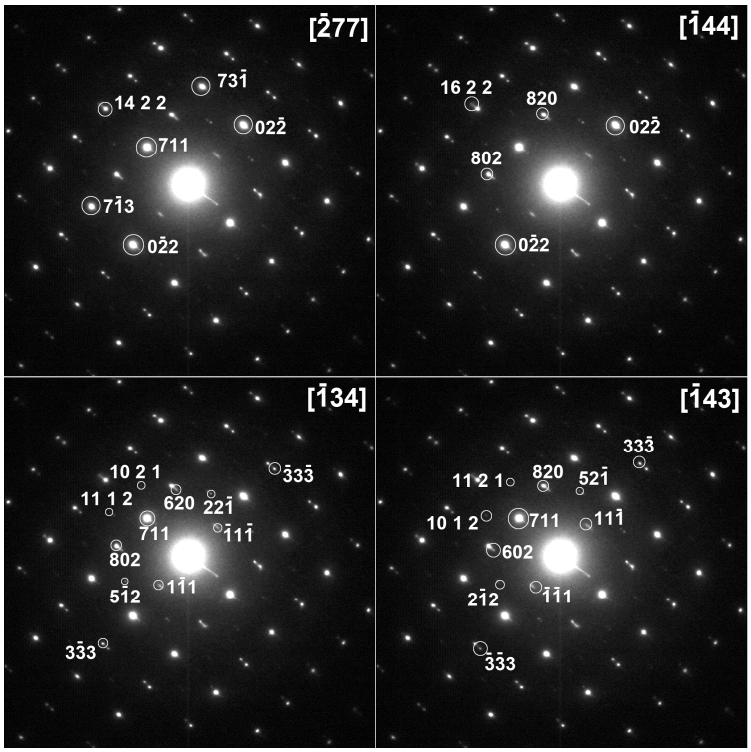

Figure S4. First PED pattern from which the reflection intensities were extracted. The pattern is an overlap of zones [-277], [-144], [-134] and [-143]. Reflections are only indexed in the pattern bearing the label of the zone they belong to.

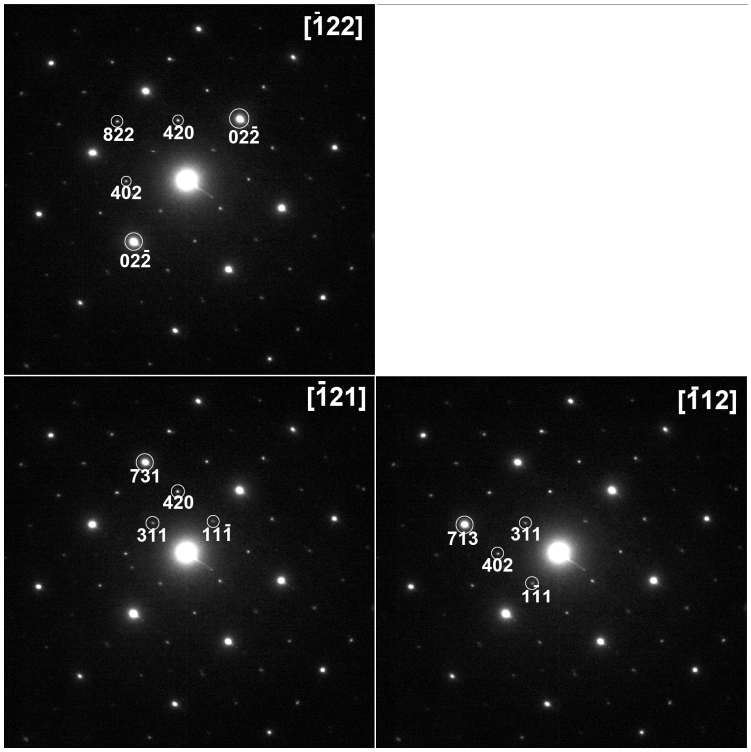

Figure S5. Second PED pattern from which the reflection intensities were extracted. The pattern is an overlap of zones [-122], [-121] and [-112]. Reflections are only indexed in the pattern bearing the label of the zone they belong to.

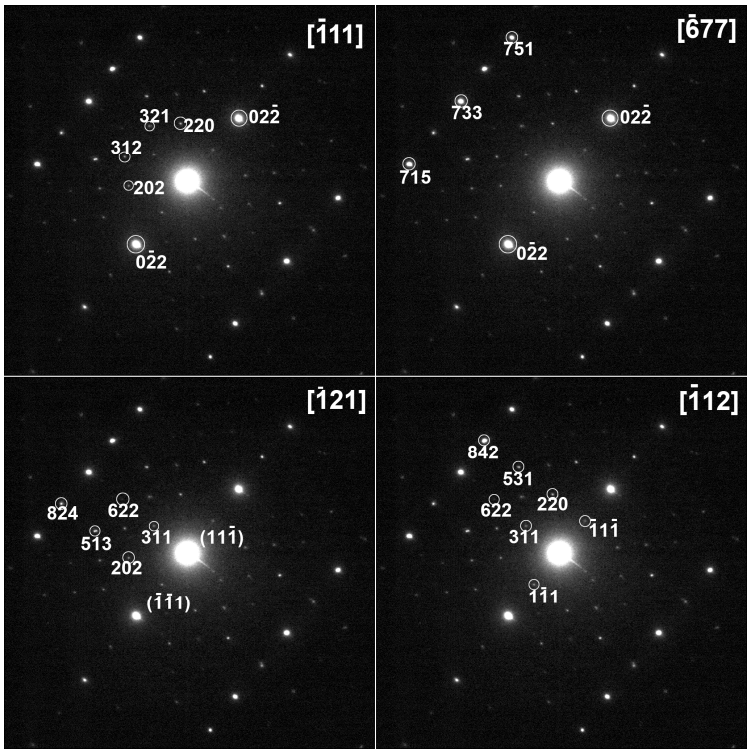

Figure S6. Third PED pattern from which the reflection intensities were extracted. The pattern is an overlap of zones [-111], [-677], [-121] and [-112]. Reflections are only indexed in the pattern bearing the label of the zone they belong to. Note that the bottom two are the same zones as for Figure S5, however, different reflections belonging to these zones are excited because of a different tilt angle relative to perfect orientation of these zones.

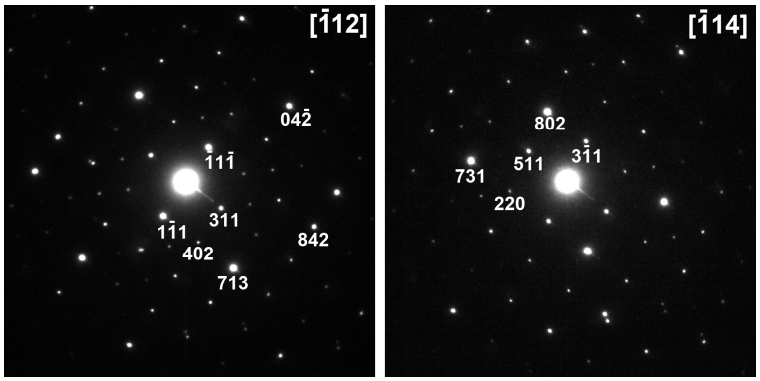

Figure S7. Fourth and fifth PED patterns from which the reflection intensities were extracted. These patterns are pure patterns. The reflections could be extracted in an automated way from these two last patterns.

Statistics on the quality of the PED data that was used

Table S1. Zones from which the reflections were used, R_{sym} for each zone ($R_{sym} = \frac{\sum_{hkl} \left| |F_{obs}(hkl)| - |F_{average}(hkl)| \right|}{\sum_{hkl} |F_{average}(hkl)|}$) where the sum runs over all observed reflections and $F_{average}$ is the average between unique reflections. The first three are extracted through 2D maps, the last two in the conventional manner.

zone	**R_{sym}***	**Unique/all**
$[\bar{2}77]$ and $[\bar{1}44]$	7.5	16/24
$[\bar{5}99]$	6.6	15/24
$[\bar{5}66]$	8.2	18/29
$[\bar{1}1\bar{1}]$	2.9	66/75
$[\bar{1}13]$	3.8	58/73